An Empirical Investigation of Convective Planetary Boundary Layer Evolution and Its Relationship with the Land Surface

JOSEPH A. SANTANELLO JR. AND MARK A. FRIEDL

Department of Geography, Boston University, Boston, Massachusetts

WILLIAM P. KUSTAS

Hydrology and Remote Sensing Laboratory, U.S. Department of Agriculture, Beltsville, Maryland

(Manuscript received 11 May 2004, in final form 8 December 2004)

ABSTRACT

Relationships among convective planetary boundary layer (PBL) evolution and land surface properties are explored using data from the Atmospheric Radiation Measurement Program Cloud and Radiation Test Bed in the southern Great Plains. Previous attempts to infer surface fluxes from observations of the PBL have been constrained by difficulties in accurately estimating and parameterizing the conservation equation and have been limited to multiday averages or small samples of daily case studies. Using radiosonde and surface flux data for June, July, and August of 1997, 1999, and 2001, a conservation approach was applied to 132 sets of daily observations. Results highlight the limitations of using this method on daily time scales caused by the diurnal variability and complexity of entrainment. A statistical investigation of the relationship among PBL and both land surface and near-surface properties that are not explicitly included in conservation methods indicates that atmospheric stability in the layer of PBL growth is the most influential variable controlling PBL development. Significant relationships between PBL height and soil moisture, 2-m potential temperature, and 2-m specific humidity are also identified through this analysis, and it is found that 76% of the variance in PBL height can be explained by observations of stability and soil water content. Using this approach, it is also possible to use limited observations of the PBL to estimate soil moisture on daily time scales without the need for detailed land surface parameterizations. In the future, the general framework that is presented may provide a means for robust estimation of near-surface soil moisture and land surface energy balance over regional scales.

1. Introduction

During the course of the day, the effects of the earth's surface radiation and energy balances are felt throughout the lower atmosphere. Turbulence and convection act to transport and mix heat and moisture within a region of the lower troposphere of variable depth known as the planetary boundary layer (PBL). The daytime (or convective) PBL is directly affected by interactions at the land surface and serves as a "short-term memory" of land surface processes on diurnal time scales (Stull 1988). As a result, the time evolution of atmospheric temperature and humidity profiles in the PBL and turbulent fluxes and temperature and moisture conditions at the land surface are dependent upon (and feed back on) one another.

One question yet to be resolved in studies of these interactions is how conditions and fluxes at the land surface can be diagnosed using observations of the PBL and its diurnal evolution. The need for this type of approach has become evident in light of the many challenges involved in measuring PBL energy budgets and modeling land–atmosphere interactions via soil–vegetation–atmosphere transfer schemes. Further, atmospheric forecast models at regional to global scales require accurate representation of surface energy and water budgets, and estimating these processes at scales applicable to such models using point-scale observations or models is a major challenge. A key hypothesis of this work is that by using the well-mixed PBL as an

Corresponding author address: Dr. Joseph A. Santanello Jr., Earth System Science Interdisciplinary Center, Hydrospheric and Biospheric Sciences Laboratory, Code 614.3, NASA-GSFC, Greenbelt, MD 20771.
E-mail: sntnello@hsb.gsfc.nasa.gov

integrated diagnostic of land surface conditions and fluxes, it may be possible to estimate regional-scale land surface fluxes without the need for specification of soil and vegetation properties, upscaling procedures, or in situ flux measurements.

Previous efforts to obtain land surface information from PBL observations have relied on in situ measurements of the PBL (Betts and Ball 1994), a combination of PBL and land surface data through conservation principles (Kustas and Brutsaert 1987), and 1D modeling of the PBL (Diak and Stewart 1989; Diak 1990; Diak and Whipple 1993, 1994). Each of these methods is constrained by the general paucity of detailed measurements of the PBL and incomplete treatment of the controls, relationships, and feedbacks between the PBL and the land surface.

With these issues in mind, the objectives of this paper are 1) to improve understanding of the factors controlling convective PBL evolution and 2) to develop methods of estimating surface conditions and fluxes from measurement of PBL evolution, focusing on observable properties of the PBL and the land surface rather than models of complex processes. The emphasis is on *daily* variability in these properties, using the PBL as an integrator of surface conditions at *regional* scales.

2. Background and previous studies

a. Conservation of heat in the PBL

Previous attempts to exploit PBL–land surface relationships have focused on closure of heat, water vapor, and carbon dioxide budgets in the PBL, but there has been little application of conservation principles to a large sample of individual days and little consensus regarding the treatment of some of the components involved (e.g., entrainment and advection), and available methods require many parameterizations, assumptions, and in situ measurements of PBL properties. These issues need to be addressed before daily surface fluxes and properties such as soil water content can be diagnosed operationally from PBL variables.

The conservation of heat in the PBL is represented by

$$\frac{\partial \overline{\theta}}{\partial t} + \frac{\overline{U_j}\partial \overline{\theta}}{\partial x_j} = \frac{\nu_\theta \partial^2 \theta}{\partial x_j^2} - \frac{1}{\overline{\rho} C_p}\left(L_v E - \frac{\partial \overline{R_{nj}}}{\partial x_j}\right) - \frac{\partial(\overline{u_j' \theta'})}{\partial x_j}, \tag{1}$$

where θ is potential temperature, t is time, U_j is mean wind speed in the jth direction, ν_θ is molecular thermal diffusivity, C_p is specific heat of moist air, ρ is air density, L_v is latent heat of evaporation, E is flux of latent heat from the surface to the atmosphere, R_{nj} is net radiation in the jth direction, and u_j' and θ' are the turbulent wind and temperature components (Kustas and Brutsaert 1987), respectively, which represent the vertical fluxes of sensible heat.

The first term in Eq. (1) ($\partial\theta/\partial t$) is the storage of heat, or time rate of change of potential temperature in the PBL through the depth of the developing PBL. The remaining terms represent the sources and sinks of this heat. Heat storage is calculated as the cumulative change in potential temperature between successive soundings from the surface to the top of the PBL (Fig. 1). PBL height (h) can be identified by visual inspection of soundings at the level of sharp increase in θ with height, but, to eliminate subjectivity here, the top of the boundary layer was identified as the level at which vertical gradients in θ exceeded a prescribed threshold (0.02 K m^{-1}).

For this work, preliminary efforts to estimate heat storage revealed that using mixed layer averages of θ (e.g., Peters-Lidard and Davis 2000; Arya 2001) leads to errors in storage estimates of more than 20% in some cases. Therefore, a numerical summation procedure was followed in which the storage term was computed from the temperature change in each 10-m layer of the PBL. This technique utilized the full vertical resolution of radiosonde data, and errors in calculating storage were on the order of only 1%–2% for typical convective PBL conditions.

The second term in Eq. (1) is advection ($U\partial\theta/\partial x$). Within the well-mixed PBL, vertical gradients of θ are small, and so vertical advection is typically not a significant contributor to heat budgets (Betts and Ball 1994). Any significant advection of heat in the vertical direction occurs near h and is accounted for in the entrainment term. Further, the effects of large-scale subsidence are negligible in comparison with vertical motions attributed to highly convective conditions (Hipps et al. 1994; Diak and Whipple 1993). Horizontal advection remains significant, and numerous methods to estimate this term have been developed. These methods include 1) using a synoptic network of radiosonde data (Kustas and Brutsaert 1987; Barr and Strong 1996; Peters-Lidard and Davis 2000), 2) using a regional atmospheric model (Diak and Whipple 1994; Barr and Betts 1997), 3) computing advection as the residual term of the conservation equation (Dolman et al. 1997), 4) assuming advection to be zero for multiday composites (Betts and Ball 1994, Betts and Barr 1996; Barr and Strong 1996), and 5) assuming advection to be negligible (Culf 1993; Hubbe et al. 1997; Yi et al. 2001).

Omitting advection from the conservation equation

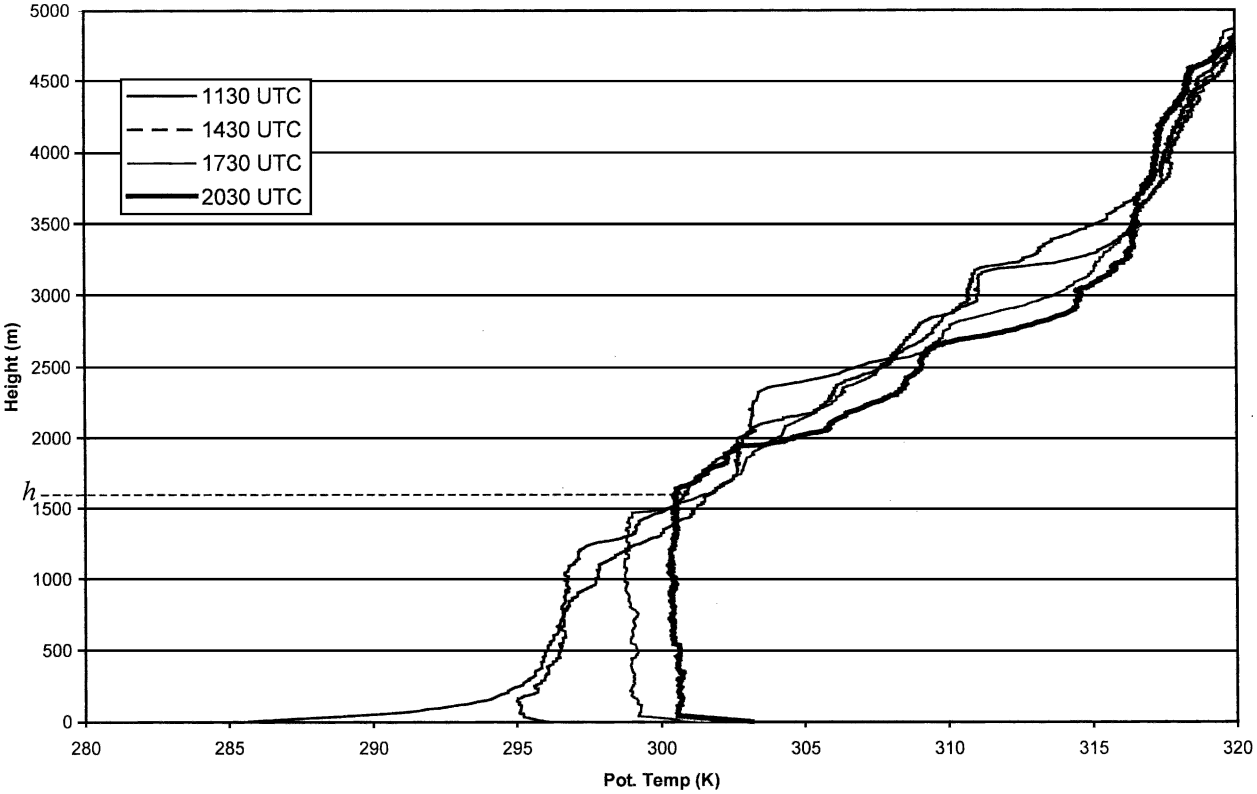

FIG. 1. Profiles of potential temperature taken from radiosonde soundings at the Lamont, OK, ARM-SGP site on 5 Jun 1997. The launch times correspond to 0630, 0930, 1330, and 1630 local time. Also labeled is the maximum height of the PBL (h).

can result in significant overestimation of sensible heating during warm advection and vice versa. Synoptic networks and regional-scale models have provided mixed results and are generally not practical for operational estimates of this term. Further, some studies have found that inclusion of advection estimates does not generally improve results, regardless of the estimation procedure that is employed (Diak and Whipple 1993; Lhomme et al. 1997; Peters-Lidard and Davis 2000). Thus, there appears to be no consensus on how to treat advection at scales of 10–200 km in the PBL, and this term represents a source of uncertainty in conservation analyses.

For this work, we used an approach to estimate horizontal advection based on the change in potential temperature in the free atmosphere (Swiatek 1992; Hipps et al. 1994; Diak and Whipple 1994; Lhomme et al. 1997; Peters-Lidard and Davis 2000). This method assumes that advection is maximum near the top of the PBL, decreasing to 30% of the maximum at the land surface, with linear variation between these two levels. This assumption accounts for a reduction of wind speed near the surface from friction and the decoupling of flow patterns in the PBL. Also inherent in this estimate is the effect of large-scale subsidence (warming) above the PBL, which has been shown to have little effect on heat budgets (Hipps et al. 1994; Diak and Whipple 1993).

The third term in Eq. (1) ($\nu_\theta \partial^2\theta/\partial x_j^2$) represents molecular diffusion of potential temperature and is orders of magnitude smaller than the other terms in Eq. (1) (Stull 1988). The fourth term ($L_v E$) represents body sources of heat that affect the entire volume of interest. For clear skies, large-scale condensation and evaporation processes are negligible within the PBL. As a result, neither of these terms is included in this analysis.

The fifth term, radiative flux divergence (RFD; $\partial R_n/\partial x_j$), is often assumed to be negligible during the daytime (Arya 2001). Glazier et al. (1976), Kustas and Brutsaert (1987), Peters-Lidard and Davis (2000), and Freedman et al. (2001), however, all emphasize the possible significance of RFD, which may be up to 40% of the total heat budget under certain conditions. To examine this issue, we used a radiative transfer model to estimate RFD in the PBL and to assess the significance of this term in the overall heat budget. "Streamer" (Key and Schweiger 1998) is a robust radiative transfer

model that includes 2-, 4-, 8-, and 16-stream approximations to the full radiative transfer equation. Atmospheric profiles of pressure, θ, and specific humidity q are required as inputs along with the surface temperature, albedo, and emissivity. Streamer simulates net radiation R_n at a prescribed set of input levels, from which the RFD can be computed by taking the difference in R_n between the top of the PBL and the land surface. Using this approach, Streamer was run for individual days at multiple sounding times to examine the daytime evolution and the response of radiative fluxes to different surface and atmospheric conditions.

The final terms in Eq. (1) $[\partial(u_j\theta)/\partial x]$ are the sensible heat flux into the PBL from the land surface and from the free atmosphere, H_s and H_i, respectively. The former is measured routinely only during short-term field experiments or by sparse measurement networks, and measurements of H_s commonly have uncertainties of 10% or more from instrument and sampling errors. Further, point measurements of surface fluxes are not necessarily representative of areas larger than the local field in which they are collected, and instrumentation to measure such fluxes is expensive and labor intensive (e.g., Smith et al. 1992). As a result, the conservation method has often been used to estimate H_s given parameterizations of the remaining terms.

The final source of heat in the PBL that must be considered is entrainment H_i. This flux of heat from the free atmosphere into the PBL is difficult to measure directly. It can be estimated using gradients of temperature and moisture at or near the top of the PBL, but such methods require numerous assumptions. For example, Culf (1993) used a simple entrainment estimate based on the jump in temperature from the mixed layer to the free atmosphere and the rate of PBL growth. This technique is based on the "slab" model developed by Tennekes (1973) and is a simplification of Eq. (1) that ignores advection, subsidence, and radiation. It is also sensitive to small errors in h (on the order of 60 m) and uncertainty in inversion-level temperature, humidity, and vertical velocity (Cleugh et al. 2003).

b. Other models and methods

Because of the difficulties in estimating many of the conservation terms, alternative techniques have been developed to infer surface fluxes from PBL observations. The simplest of these techniques, the "encroachment" method (equating $d\theta/dt$ to H_s alone), almost always overestimates sensible heat flux because it does not account for heat added to the PBL through other processes such as entrainment, advection, and radiation (Swiatek 1992). Even under highly convective conditions, the proportion of heat added to the PBL from surface heating rarely exceeds 70% (Driedonks 1982; Stull 1988). Hubbe et al. (1997) applied this method to three days in the central Great Plains in 1995 with little success.

Because of these limitations, much work has been done to develop parameterizations for entrainment as a function of surface sensible heat flux:

$$-H_i = A_R H_s. \tag{2}$$

For multiday averages, values for entrainment parameter A_R in the literature vary from 0.20 to 0.54 (Stull 1988; Betts and Ball 1994; Betts and Barr 1996; Barr and Strong 1996; Barr and Betts 1997; Dolman et al. 1997; Peters-Lidard and Davis 2000; Margulis and Entekhabi 2004), and hourly values range from -0.2 to greater than 2.0 (Kustas and Brutsaert 1987; Peters-Lidard and Davis 2000; Cleugh et al. 2003). An accurate estimate of this parameter would enable entrainment to be specified without the need for detailed measurements in the PBL, but agreement on daily or hourly average values has proven difficult. Pino et al. (2003) used large-eddy simulation to include the role of mechanical turbulence and shear on entrainment. Of significance is that they show that wind shear near the surface and at the inversion contributes to entrainment and that A_R should be adjusted depending on the wind speed. For highly convective and shearing conditions, Pino et al. (2003) suggest that A_R should be close to 0.45. Because of difficulties involved in parameterizing and measuring entrainment, here we estimate this term as a residual of the conservation equation.

3. Study site and data

The Atmospheric Radiation Measurement Program Cloud and Radiation Test Bed in the southern Great Plains (ARM-SGP) provides surface flux, meteorological, and hydrological observations along with atmospheric profiles for a network of sites in and near the winter-wheat belts of Oklahoma and Kansas. This experiment has been widely used in previous studies (information on the site locations and characteristics was available online at http://www.arm.gov/sites/sgp.stm).

a. Radiosonde and surface data

Radiosondes were launched daily at 1130, 1430, 1730, and 2030 UTC (0630, 0930, 1230, and 1530 local time) at the ARM-SGP central facility (Lamont, Oklahoma) during intensive field campaigns in June, July, and August of 1997. In 1999 and 2001, radiosondes were

launched a minimum of two times daily (1130 and 2030 UTC) during the same months. Soundings at 1130 and 2030 UTC are representative of the onset of surface heating and maximum h, respectively, and serve as ideal endpoints for computing daily averages of PBL variables. More detail on the radiosonde sensors, measurements, and calibrations at the ARM-SGP sites can be found in Hubbe et al. (1997). For this work, radiosonde measurements of temperature, dewpoint, and pressure were converted to profiles of θ and q (using standard thermodynamic relationships) that extend well above the PBL, up through 25 000 m.

ARM-SGP employs both Bowen ratio (EBBR) and eddy correlation (ECOR) instruments that provide 30-min average fluxes of net radiation and sensible, latent, and soil heat, along with collocated surface radiant temperature, soil water content, 2-m air temperature, mixing ratio, and wind measurements from micrometeorological instrumentation. At the Lamont facility (CF-13), the ECOR instrumentation is located along an east–west fence line that separates wheat and grasslands and is in close proximity to concrete, housing, and instrumentation to the north. Further, the ECOR data are not continuous and are known to be less reliable for the dates used in this study, and therefore they were not included in the analyses.

The EBBR instrumentation at CF-13 lies adjacent to a wheat field in open grassland. In fact, the land cover of the region surrounding CF-13 is composed mainly of alternating fields of winter wheat (34%) and grassland (29%) during the summer months. Winter wheat is harvested in the late spring, leaving fields of mostly stubble (less than 50 cm) and bare soil in its place. After analyzing data from nearby extended facilities, we chose to average the fluxes from the sites that are most representative of land cover at CF-13 and of the region as a whole. Averaging the fluxes of the three ARM-SGP sites nearest and most similar in land cover characteristics to the radiosonde launch site (CF-13, EF-15 at 100 km, and EF-9 at 75 km) helped to smooth out localized anomalies in the data, but, more important, the averaged values are representative of the 10–200-km fetch over which the land surface interacts with the PBL (Oke 1987; Stull 1988; Dolman et al. 1997; Peters-Lidard and Davis 2000; Cleugh et al. 2003; Ek and Holtslag 2004).

Although not included explicitly in the conservation equation, atmospheric stability and soil moisture are strongly related to the growth of the convective PBL. Stability $\gamma_\theta(z)$ is defined as the change in potential temperature with height and is very sensitive to the depth in which it is measured. Previous studies and models include consideration for the free-atmosphere stability (Driedonks 1982; Arya 2001) and the strength of the inversion, but, from an intuitive perspective, the initial stability *within* the layer of PBL growth (γ_{ml}) is a more significant control on how quickly and deeply the PBL grows. Findell and Eltahir (2003) highlight the importance of three components of morning atmospheric profiles: 1) the strength of the nocturnal inversion near the surface, 2) the stability from the top of the nocturnal inversion to the height of the previous day's PBL, and 3) the strength of the gradient from the top of the mixed layer to the free atmosphere. These three features are directly accounted for in our measure of γ_{ml}, which was estimated from the morning (1130 UTC) sounding as the gradient in potential temperature from the nocturnal surface inversion to the maximum height of the previous day's PBL.

Soil moisture probe measurements were collected at five sampling locations distributed across a 10-m area at each of the three flux sites. To provide representative soil moisture conditions across the region, half-hourly values of volumetric soil moisture w at 2.5-cm depth were averaged for each day across the five sensors at each location and then were averaged across the three flux sites. Within the study period, there were several well-defined "dry downs," capturing a full range of w from near-saturated (0.35 $m^3\ m^{-3}$) to desiccated ($<$0.10 $m^3\ m^{-3}$) conditions.

b. Data selection

Data for the summer (June, July, and August) of 1997, 1999, and 2001 were characterized by high available energy at the land surface and a wide range of boundary layer heights. In addition, there were numerous precipitation events and complete dry-down cycles of the soil. Atmospheric profiles that behaved erratically or showed signs of a frontal passage or strong advection were removed. Overall, 132 days of data were used in the analyses.

4. Results

a. Composite profiles

Figure 2 presents composite profiles of θ and q for three summers (1997, 1999, 2001) of ARM-SGP radiosonde data. Composites were generated by averaging the 1130 and 2030 UTC daily profiles of θ and q and then scaling them to the mean PBL height of each year. The top of the PBL is clearly detectable from the 2030 UTC radiosonde data, even when averaged over a 3-month period. Table 1 presents the mean values of

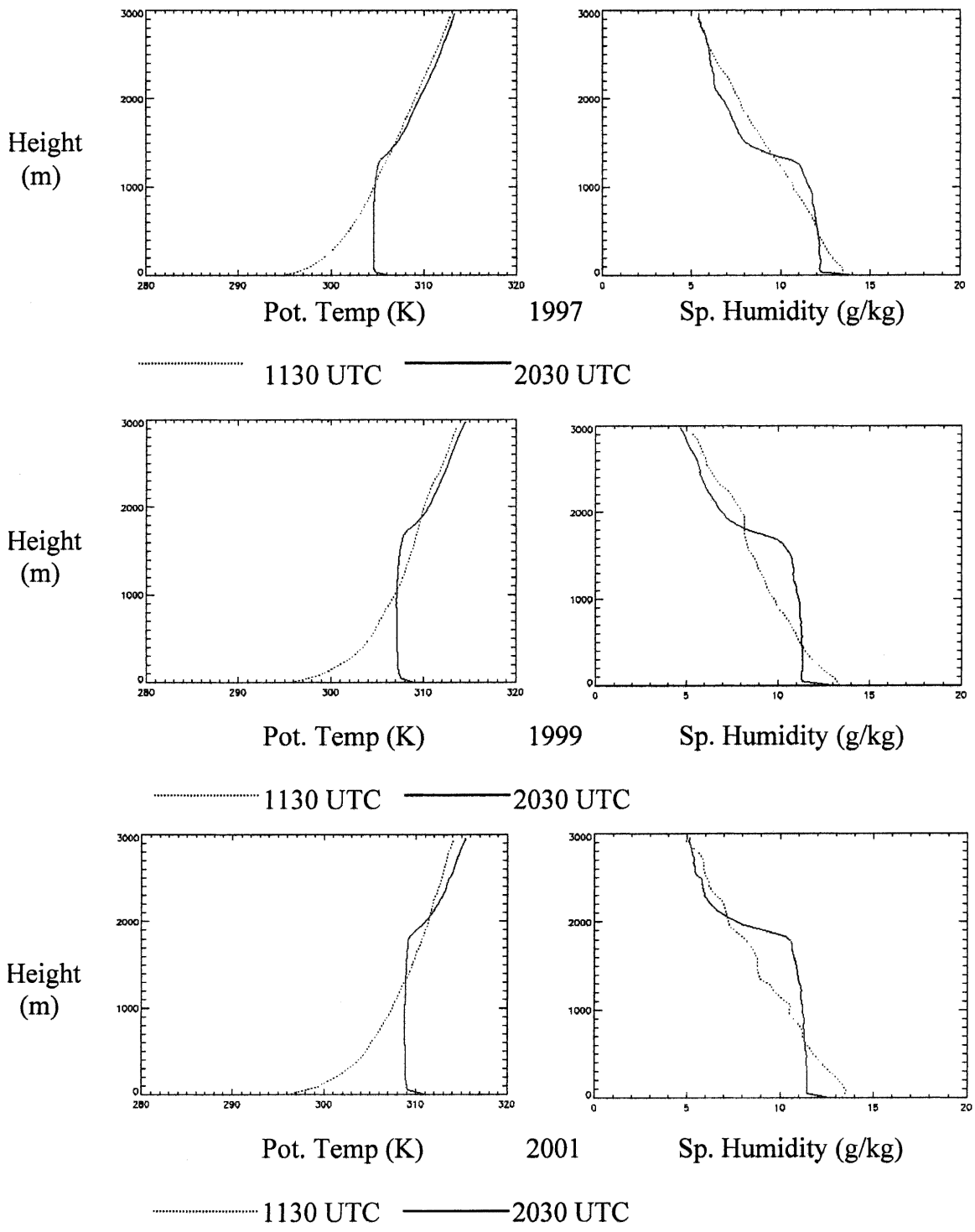

FIG. 2. Composite profiles of (left) potential temperature and (right) specific humidity calculated from daily radiosonde soundings at Lamont, OK, during three summers: (top) 1997, (middle) 1999, and (bottom) 2001.

related PBL and land surface variables for each summer. As expected, h is negatively correlated with average daily w and initial γ_{ml} and is positively correlated with average daily Bowen ratio and 2-m potential temperature change $\Delta\theta_{2m}$ between 1130 and 2030 UTC. In particular, the strong control of soil moisture on h is evident in the yearly averages, and the impact of stability is apparent in the daily data (not shown).

TABLE 1. Annual average values for selected PBL and land surface variables taken from 55, 44, and 33 diurnal observations in 1997, 1999, and 2001, respectively, at the central facility of the ARM-SGP site.

	1997	1999	2001
PBL height (m)	1305	1780	1845
Stability (K m^{-1})	0.0062	0.0051	0.0060
Bowen ratio	0.41	0.48	0.72
Soil moisture (m^3 m^{-3})	0.22	0.19	0.13
2-m potential temperature change (K)	11.4	12.6	14.4

b. Radiative flux divergence

Vertical profiles of net radiation as simulated by Streamer for a representative day with clear skies and substantial PBL growth (8 July 1997) are shown in Fig. 3. This figure reveals strong diurnal variation in RFD [where RFD = R_n(top) − R_n(surface)] and illustrates how net heating in the PBL changes from cooling to warming over the course of the day. Figure 4 shows RFD within the PBL estimated from Streamer for 5 days in 1997. Diurnal variation is clearly evident and is characterized by negative values of RFD at night, maximum values near noon, and large positive RFD through the afternoon. Daily mean values of RFD range from 0 to 20 W m^{-2}, but at any single time of day RFD is much larger in magnitude (up to 90 W m^{-2}).

The primary cause of variability in daily mean RFD is water vapor because it absorbs much of the outgoing longwave radiation from the surface and acts to keep heat in the PBL. This extra heat increases net radiation at the surface, which reduces the *gradient* of net radiation from the surface to the top of the PBL (Fig. 3). Thus, the net effect is that high q near the surface reduces the magnitude of RFD throughout the day, particularly in the afternoon. In Fig. 4, for example, 23 June and 8 July were more humid (>12 g kg^{-1}) than 5 and 6 June and 12 July (<10 g kg^{-1}). To incorporate RFD and its dependence on water vapor into conservation analyses, we used Streamer to estimate and scale the daily mean RFD for the range of specific humidities present in the dataset (7–18 g kg^{-1}).

c. Conservation analyses

PBL heat storage was computed from the early morning (1130 UTC) and midafternoon (2030 UTC) radiosonde profiles of potential temperature. As we previously described, advection was estimated based on the free-atmosphere temperature change between 1130 and 2030 UTC, average daily H_s was estimated from 30-min observations between 1130 and 2030 UTC, and

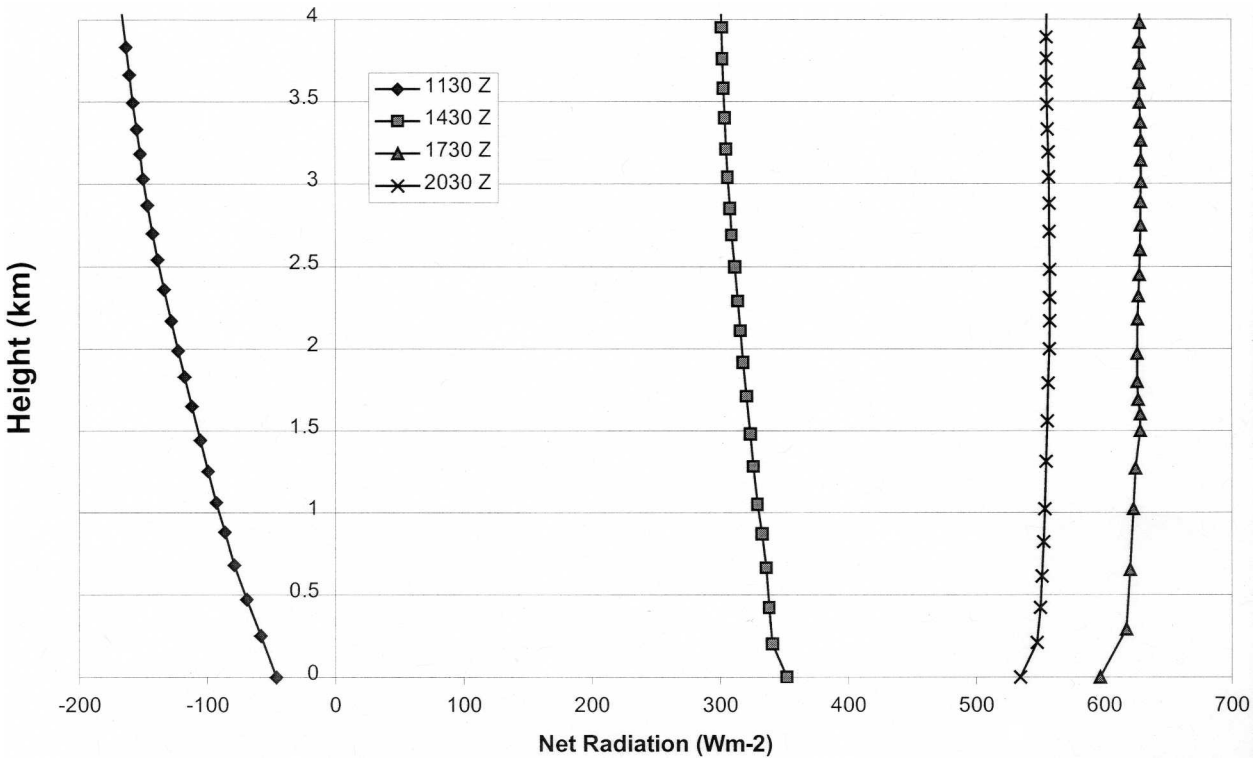

FIG. 3. Net radiation from the surface to 4 km at four different times on 8 Jul 1997 as simulated by Streamer.

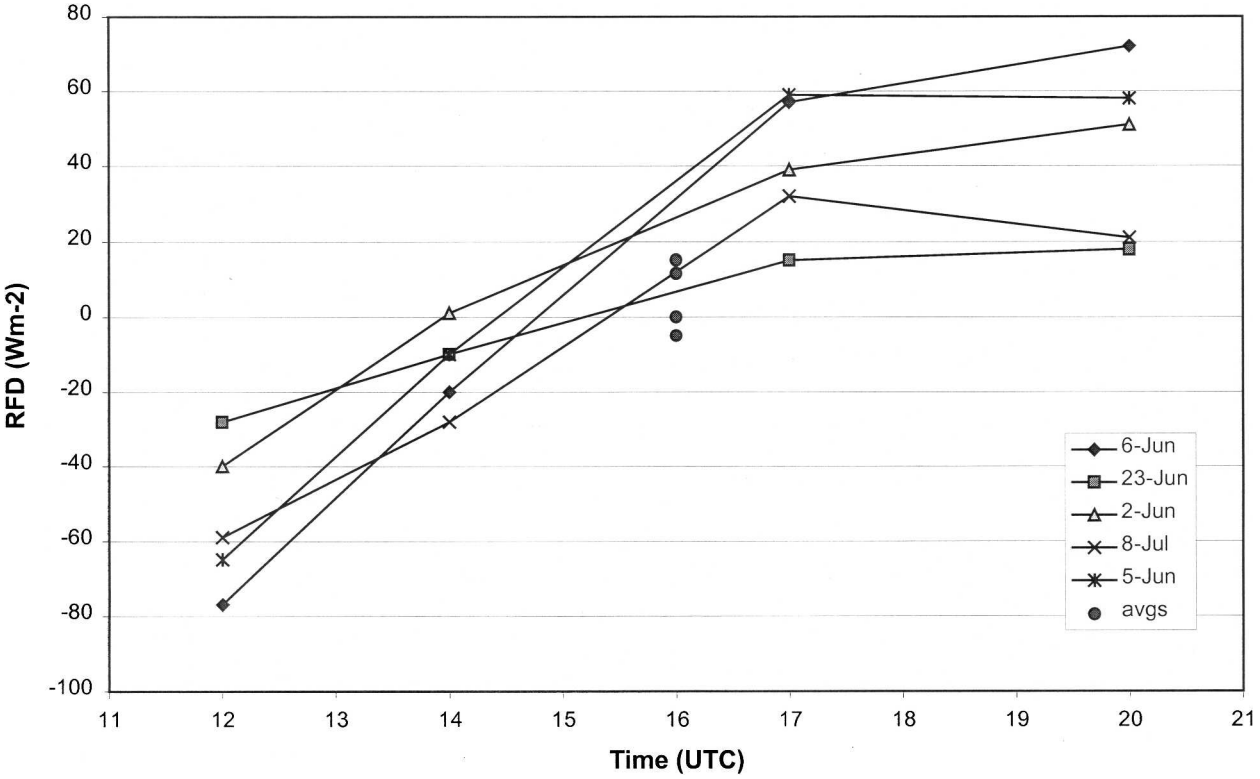

FIG. 4. Radiative flux divergence simulated by Streamer for five select days in 1997 at Lamont, OK.

average daily RFD was computed from Streamer initialized using 1130, 1430, 1730, and 2030 UTC radiosonde data. Because H_s data were available from flux towers at ARM-SGP, budget analyses were performed using observations of H_s, advection, and RFD to compute H_i as a residual for each day of the study.

Table 2 presents the measured and estimated budget terms, computed daily as described in section 4 and then averaged over each year of data. Contributions to total heat storage ranged from 1.5% to 7.8% for advection, from 2.9% to 4.3% for RFD, from 62.3% to 65.8% for H_s, and from 23.3% to 32.8% for H_i. Together, advection and RFD contribute less than 10% of the heat added to the PBL throughout the day. Also, H_s is a near-constant proportion of storage for all three years, and the absolute value of H_i changes very little from year to year.

TABLE 2. Mean budget components (W m^{-2}) estimated from each year of radiosonde and surface flux data. RFD is radiative flux divergence, H_s is sensible heat flux from the land surface to the PBL, and H_i is entrainment of sensible heat from the free atmosphere to the PBL.

Year	Days	Storage	Advection	RFD	H_s	H_i
1997	55	144.2	2.4	4.8	89.8	47.3
1999	44	164.6	8.8	6.9	104.1	44.8
2001	33	202.0	15.9	6.0	132.9	47.2

The mean value of the entrainment parameter A_R for all 132 days is 0.48, which is much larger than the widely used value of 0.20. By using this estimate of A_R in combination with the conservation equation, we can attempt to solve for H_s. To test how robust this value is, estimates of H_s derived in this manner are plotted against measured fluxes from SGP in Fig. 5. It is clear that there is little skill in predicting surface sensible heat flux (coefficient of determination $R^2 = 0.15$), which lends credence to the hypothesis that large day-to-day variability is present in the proportion of heat added to the PBL from the surface versus entrainment. This result also illustrates the poor ability of *mean* budget parameters to capture PBL variability on daily time scales using heat conservation principles.

Large estimates of A_R estimated from field experiments (ranging from 0.33 to 0.54) have been linked to high wind speeds in the PBL (Kustas and Brutsaert 1987; Betts and Barr 1996; Peters-Lidard and Davis 2000). As a result, some entrainment parameterizations include a correction for mechanical turbulence (Cleugh and Grimmond 2001) through use of the friction veloc-

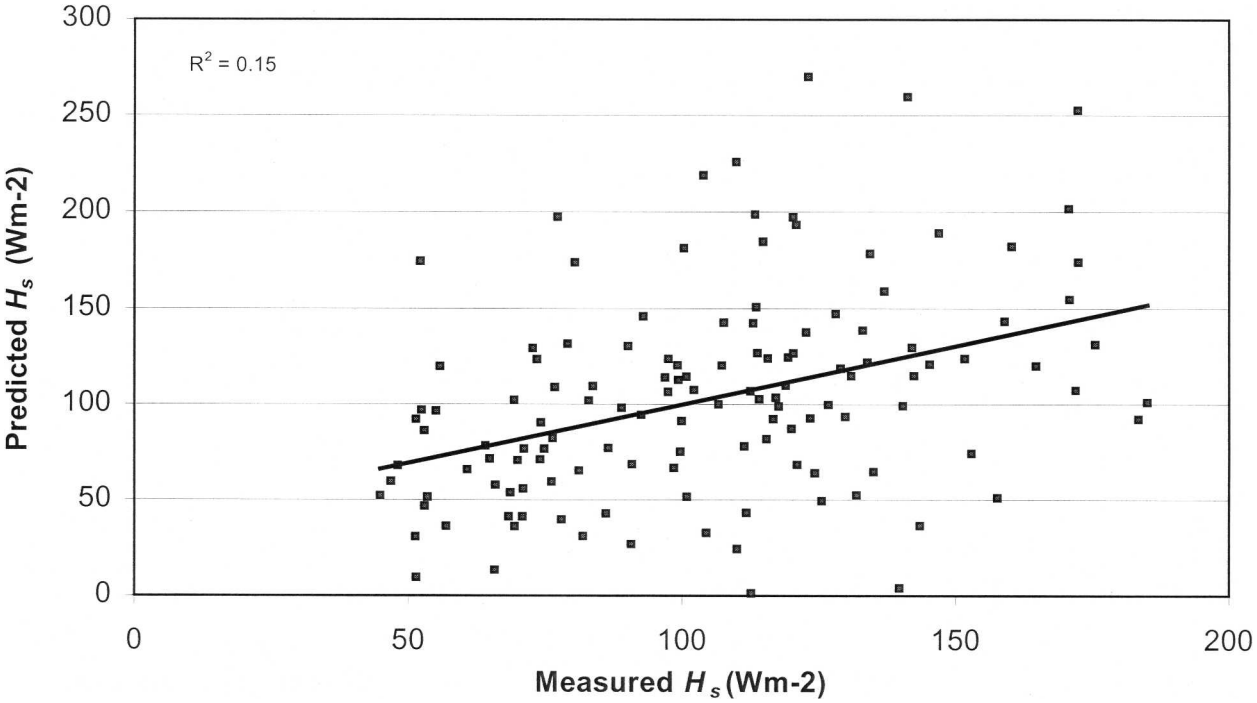

FIG. 5. Measured surface sensible heat flux vs the flux estimated using closure of the conservation equation and prescribing entrainment as 48% of the surface flux ($A_R = 0.48$).

ity u_* (the scaling parameter for mechanical turbulence). For the datasets considered in this work, the mean u_* was 0.83 m s^{-1} and the total contribution of mechanical turbulence to entrainment [$\theta_v u_*^3/(gh)$; Kustas and Brutsaert 1987] was 0.0027 K m s^{-1}, which are considerably higher than the values quoted in previous studies that suggested that A_R is closer to 0.20. Therefore, it is possible that relatively high mechanical turbulence at the ARM-SGP site may contribute to the large value for mean entrainment.

Inspection of the relationship between *daily* u_* and H_i, however, does not support a direct relationship. This result is consistent with results found by Margulis and Entekhabi (2004), who also found a weak relationship ($R^2 = 0.19$), and could explain why A_R estimates do not improve when turbulence corrections are included. Note that we have not explicitly accounted for the contribution of wind shear across the PBL inversion, which can be significant under certain conditions (sea breeze, urban, low surface heating). However, these conditions do not apply to the ARM-SGP site, and the data reveal little correlation between these terms for days with considerable wind shear (which were few) and high entrainment. In other words, high wind speeds at the ARM-SGP site may explain the large value of *mean* A_R, but the relationship on diurnal scales is confounded by other variables that affect PBL evolution.

d. First-order controls on PBL–land surface relationships

In this section, we consider how conservation processes are controlled by a number of variables, including h, γ_{ml}, w, $\Delta\theta_{2m}$, and wind speed. In particular, the relationships between processes controlling PBL evolution are captured to first order in the set of coupled equations that describe heat conservation, PBL growth, and sensible heat flux. As a consequence, variance in each of the budget terms (which are difficult to measure) should be reflected in observable properties of the PBL and land surface. For example, heat storage in the PBL (represented by the area between successive vertical profiles of θ) is primarily controlled (and bounded graphically) by h, γ_{ml}, and $\Delta\theta_{2m}$, and as a result is directly related to all three variables. In a similar way, H_s provides the majority of heat input to the PBL but is principally controlled by w, and the magnitude of entrainment is reflected in the positive correlation between $\Delta\theta_{2m}$ and h and the negative correlation between change in 2-m specific humidity Δq_{2m} and h.

Observations of γ_{ml}, w, $\Delta\theta_{2m}$, and Δq_{2m} all exhibit well-defined covariance with h (Fig. 6). In fact, over 48% of the variance in h can be explained by $\Delta\theta_{2m}$ alone. These relationships are also strongly nonlinear. For example, when γ_{ml} drops below 0.0048 K m^{-1}, h increases rapidly. A similar threshold is observed when

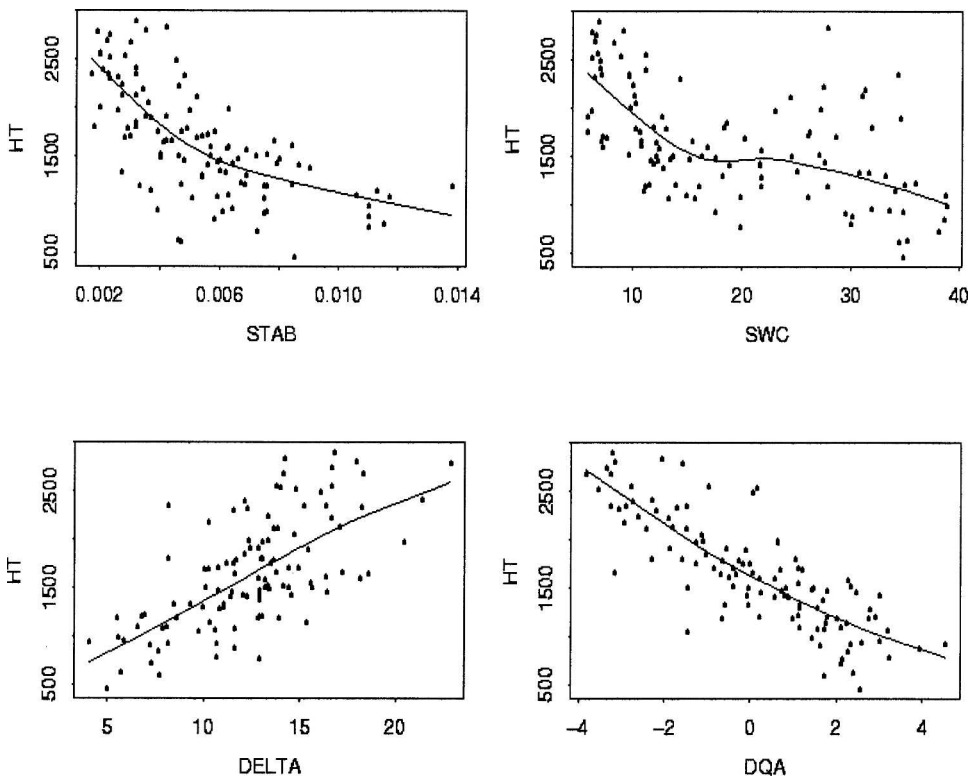

FIG. 6. Observations of stability (STAB; K m^{-1}), soil water content (SWC; $m^3\ m^{-3} \times 10^2$: percent volumetric), change in 2-m potential temperature (DELTA; K), and change in 2-m specific humidity (DQA; g kg^{-1}) plotted against the height of the PBL (HT; m) for all 132 days of the study. The lines represent local regression models fit to the data.

w drops below 0.12 $m^3\ m^{-3}$, in which case h and the surface Bowen ratio (not shown) increase sharply. These patterns reflect rapid soil drying, increased sensible heat flux, and decreased (soil limited) evaporation and are not captured by slab- or conservation-based approaches because these variables and nonlinear relationships are not included, at least directly, in such models.

Based on statistical evidence (not shown), γ_{ml} is the most important variable controlling h. In particular, initial conditions characterized by a deep unstable layer (the residual layer that forms overnight) are conducive to significant PBL growth on that day. On the other hand, although there are instances of strong convective cells initiating under a capping lid (often forming severe storms), stable atmospheres will generally restrict PBL development and act as a lid on convective cells that develop during the day, regardless of the strength of surface heating and mechanical turbulence. Such instances of very high H_s and low h are also not characterized well by traditional PBL models. These models often assume that these two variables are positively correlated, do not directly account for the effects of γ_{ml}, and mask the influences of basic properties that influence PBL growth such as w.

e. Stability and soil water content as controls

Based on the results described above, the two most influential and fundamental properties controlling the evolution of the PBL are stability and soil water content. These variables are representative of the relative strength of atmospheric and land surface control on h, respectively. Both γ_{ml} and w have a similar impact on $\Delta\theta_{2m}$, and, as we previously mentioned, h is strongly correlated with $\Delta\theta_{2m}$. To explore further the relationships among these variables, the two following functional relationships were examined:

$$h = f(w, \gamma_{ml}) \quad \text{and} \quad \Delta\theta_{2m} = f(w, \gamma_{ml}).$$

As we discussed above, w controls surface fluxes that fuel the growth of the PBL and stability restricts growth of the mixed layer and entrainment, a situation that, in turn, controls the structure of the PBL (reflected in $\Delta\theta_{2m}$).

To examine these relationships, we employed a pro-

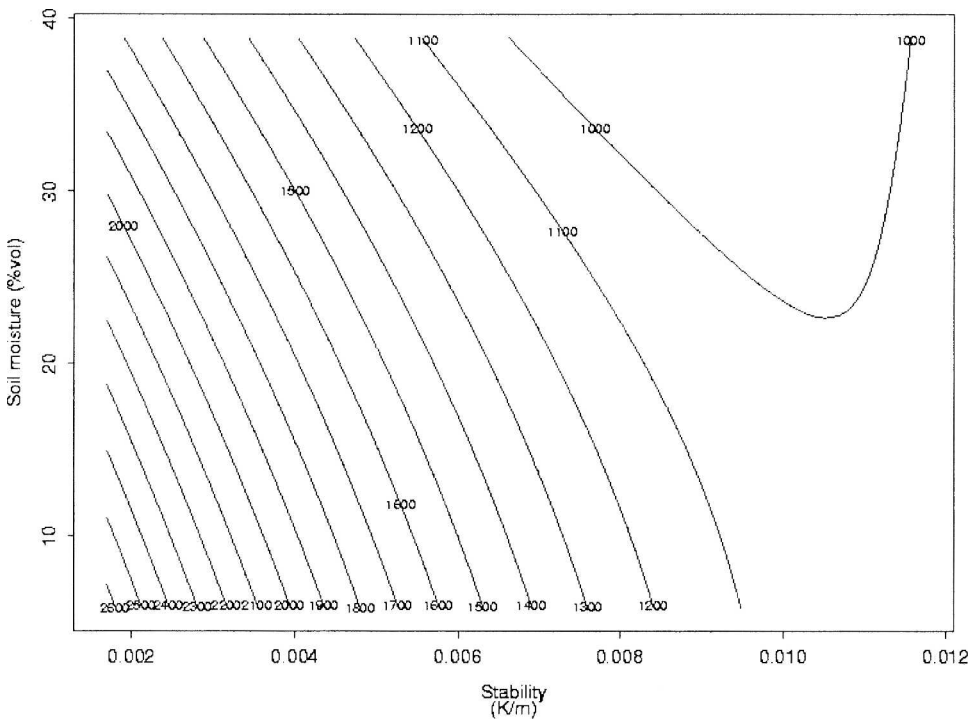

FIG. 7. PBL height (m) estimated as a function of stability and soil water content from a trend surface for all 132 days of the study. The highest heights are found under conditions of low soil water content and low stability, and vice versa.

cedure similar to the one described by Diak and Stewart (1989), Diak (1990), and Diak and Whipple (1993), who used a PBL–land surface model to simulate h and surface temperature change over a range of prescribed surface Bowen ratio and roughness. Simulated values for h were then used to estimate the surface Bowen ratio from observations of the PBL and surface temperature. In contrast, our analyses utilized only observational data and eliminated surface roughness (model parameter) and surface temperature in favor of two easily observable quantities (γ_{ml} and $\Delta\theta_{2m}$).

Using data from the ARM-SGP site, we estimated polynomial surfaces to predict h and $\Delta\theta_{2m}$ using a least squares criterion (Venables and Ripley 1999). These equations can be used to predict h and $\Delta\theta_{2m}$ as separate functions of w and γ_{ml}. Figure 7 shows h predicted using this method, with contours across the full range of γ_{ml} and w present in the dataset. This surface is the mean of 132 surfaces generated by holding 1 day out and creating a surface based on the remaining 131 days (jackknife). This surface explains 61% of the variance in h when tested against the independent data. Further, a linear model using $\Delta\theta_{2m}$ is able to explain 8% of the residual variance (i.e., together, γ_{ml}, w, and $\Delta\theta_{2m}$ explain 69% of the variance in h). A second surface (Fig. 8) predicts $\Delta\theta_{2m}$ across the same range of γ_{ml} and w and explains 51% of the variance in $\Delta\theta_{2m}$, with h explaining an additional 5%.

By combining these expressions we obtain two sets of equations with two unknowns that capture strong predictive relationships among the four variables. In this manner, any two variables can be estimated from observations of the remaining two. When using γ_{ml} and $\Delta\theta_{2m}$ as predictors, this method explains 85% of the variance in h (Fig. 9), which is a significant improvement over simple- or multiple-regression models that predict PBL height.

5. Discussion

Using the technique presented in section 4e, it is possible to estimate w from observations of h, γ_{ml}, and $\Delta\theta_{2m}$. To do this, the expressions predicting h and $\Delta\theta_{2m}$ were inverted to solve for w. A key limitation of this approach, however, is that the estimated surfaces only capture the first-order variance in the relationships among these variables. For example, the observed range of h in the dataset is 400–2900 m, but the predicted range is 1000–2700 m. As a consequence, cases in which observations of h or $\Delta\theta_{2m}$ lie at the tails of their respective frequency distributions tend to yield estimates of w that are outside of the observed range of this variable.

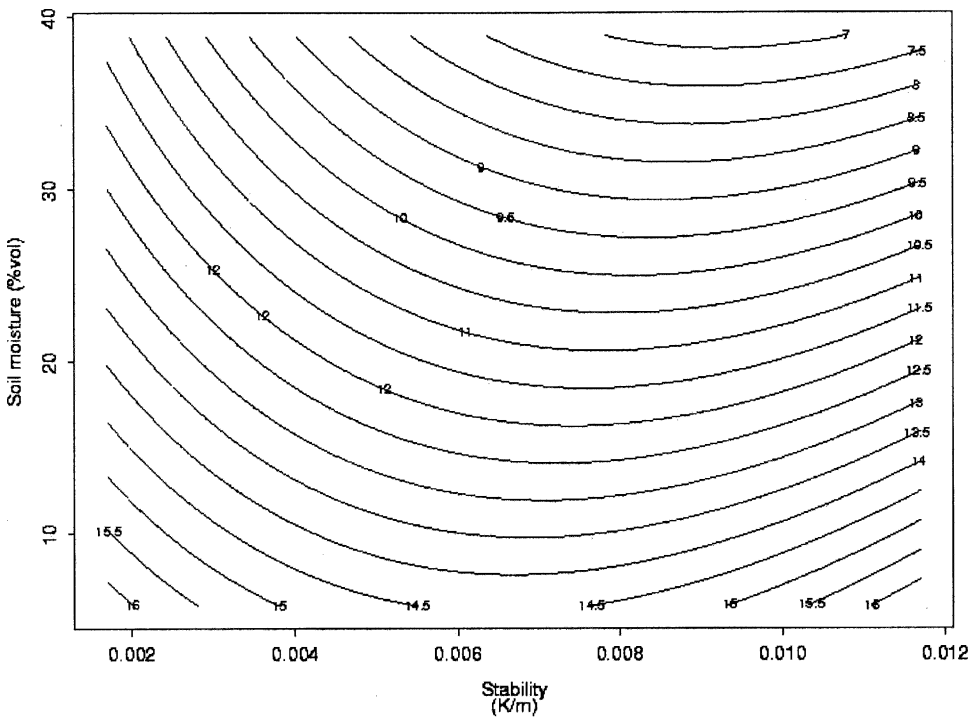

$$\Delta\theta_{2m} = 10.72 - 0.96\gamma_{ml} - 3.53\gamma_{ml}^2 + 1.94w - 1.07w\gamma_{ml} - 0.16w^2$$

FIG. 8. The 2-m potential temperature change (1130–2030 UTC; K) estimated as a function of stability and soil water content from a trend surface for all 132 days of the study. The largest temperature changes are found under conditions of low soil water content, and vice versa.

To account for this limitation, we transformed the soil moisture data in a fashion that both minimizes this problem and is also reasonable from a physical perspective. To do it, we assumed that h is relatively insensitive to w beyond the range of saturation and wilting points for soil moisture. Based on the range of w observed at the SGP site and reference values for the soil types in the SGP region (Clapp and Hornberger 1978), soil moisture values at saturation and wilting point were prescribed to be 0.45 and 0.03 $m^3\ m^{-3}$, respectively. Predictions for w that were greater than the observed maximum (0.38 $m^3\ m^{-3}$) were rescaled linearly to lie between 0.38 and 0.45 $m^3\ m^{-3}$. In a similar way, those that were lower than the observed minimum (0.06 $m^3\ m^{-3}$) were rescaled between 0.03 and 0.06 $m^3\ m^{-3}$. Predictions for w based on this approach are plotted in Figs. 10a,b and are highly correlated ($R^2 = 0.67, 0.63$) with the original w data using the independent tests described in section 4e. Further, if the data are averaged across 5% intervals of volumetric soil moisture (which corresponds to the approximate accuracy of soil moisture measurements), R^2 increases to 0.91.

Considerations of scale are also central to the results presented in this paper. The PBL integrates surface properties and fluxes over spatial scales (10–100 km) that are much different from the scales at which the surface data were collected (point scale). Therefore, the representativeness of the surface data vis-à-vis the estimated boundary layer budgets is a critical issue that affects the reliability of the results from this analysis. To explore this issue, we examined the correlation of h with H_s and w, both at individual stations and across all of the three stations included in the analyses.

At individual stations, H_s is highly correlated with w (correlation coefficient $r = 0.59$, 0.52, and 0.58). When H_s and w are averaged over all three sites, however, the correlation decreases substantially ($r = 0.32$). At the same time, h is more highly correlated with spatially averaged measurements of H_s and w ($r = 0.45$ and $r = 0.47$) than it is with measurements at individual stations ($r = 0.33$, 0.26, and 0.27 and $r = 0.36$, 0.30, and 0.38). These results demonstrate that, at the scale of individual flux stations, the surface Bowen ratio is strongly controlled by local soil moisture and that averaging these variables across multiple stations tends to decrease the correlation between w and H_s. At the scale of the PBL, however, the lower atmosphere responds to flux quantities that are integrated over much larger spa-

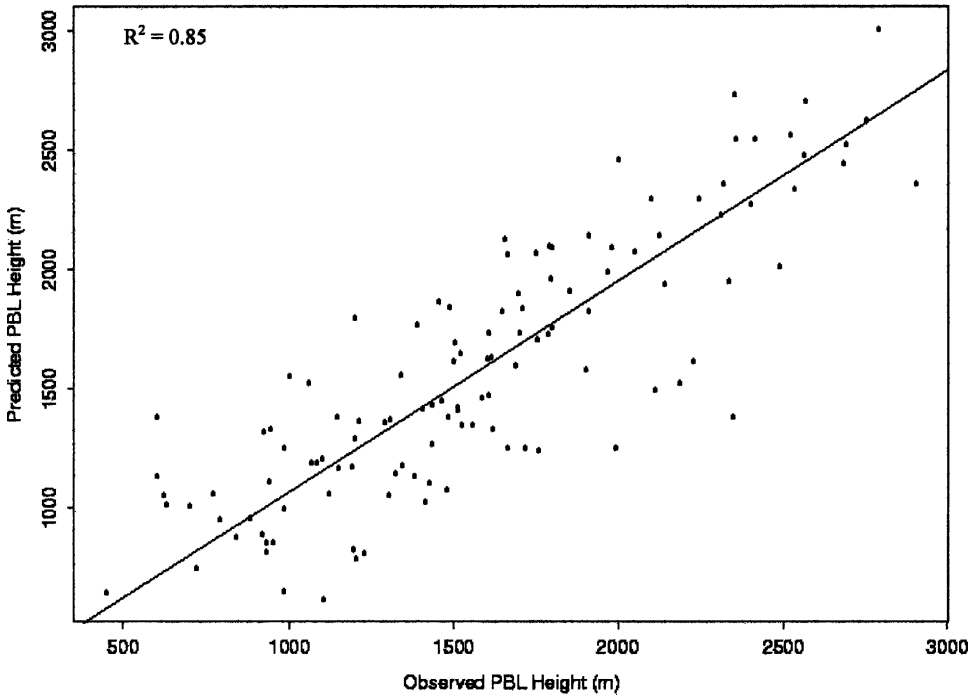

FIG. 9. Observed PBL height h vs that predicted using the trend surface in Fig. 7 and 132 daily observations of stability, soil water content, and 2-m potential temperature change.

tial scales, and thus the spatially averaged fluxes correlate well with h. In the absence of a denser network of ground sites, it is impossible to assess fully the "representativeness" of the H_s and w data vis-à-vis the radiosonde data used to compute the boundary layer budgets. The area-averaged relationships between h and both w and H_s are significantly stronger than those observed at any single site, however, which supports the approach used here.

It is also interesting to note that the data show a stronger relationship between h and w than between h and H_s. Because h is primarily controlled by the energy budget of the PBL (and not soil moisture), this result is somewhat counterintuitive. We hypothesize that this result reflects a key difference in the nature of these two variables: soil moisture provides a slow-response variable that integrates surface processes over longer time periods than the surface flux data and can provide a useful diagnostic regarding the longer-term state (or "memory") of land–atmosphere coupling relative to hourly or daily average values for surface fluxes. Because soil moisture measurements incorporate a memory of preceding land–atmosphere fluxes (which H_s does not), we observed higher correlation in this work between h and w than for h and H_s. The simplicity of the method presented above to obtain a bulk surface moisture product could make it useful for a variety of atmospheric and hydrologic modeling applications at regional or larger scales.

One of the main goals of this research was to improve understanding of PBL–land surface interactions, particularly where conservation approaches are limited and where models of PBL growth and land surface energy balance break down. One such instance occurs when rapid and large PBL growth is underpredicted using slab models, and our results show that this limitation is likely related to stability and soil moisture conditions: once the soil has dried ($w < 0.13$ m^3 m^{-3}), surface heating forces the PBL to grow larger each day. As it does, a deeper and stronger residual layer forms each night (lowering the γ_{ml} of the following day), which further encourages PBL growth regardless of the magnitude of H_s. This cycle continues until rainfall occurs or PBL development is constrained by another component of the system (subsidence, thick cloud cover, or weak winds). This positive feedback explains the tendency for rapid PBL development under conditions in which w and γ_θ are both low, and why conventional PBL growth models based on H_s tend to break down under such conditions. This also suggests that during extended dry-downs of the soil, h determines the residual layer depth, and, by extension, is correlated to the γ_{ml} and h of the following day.

Last, the results presented in this work suggest that

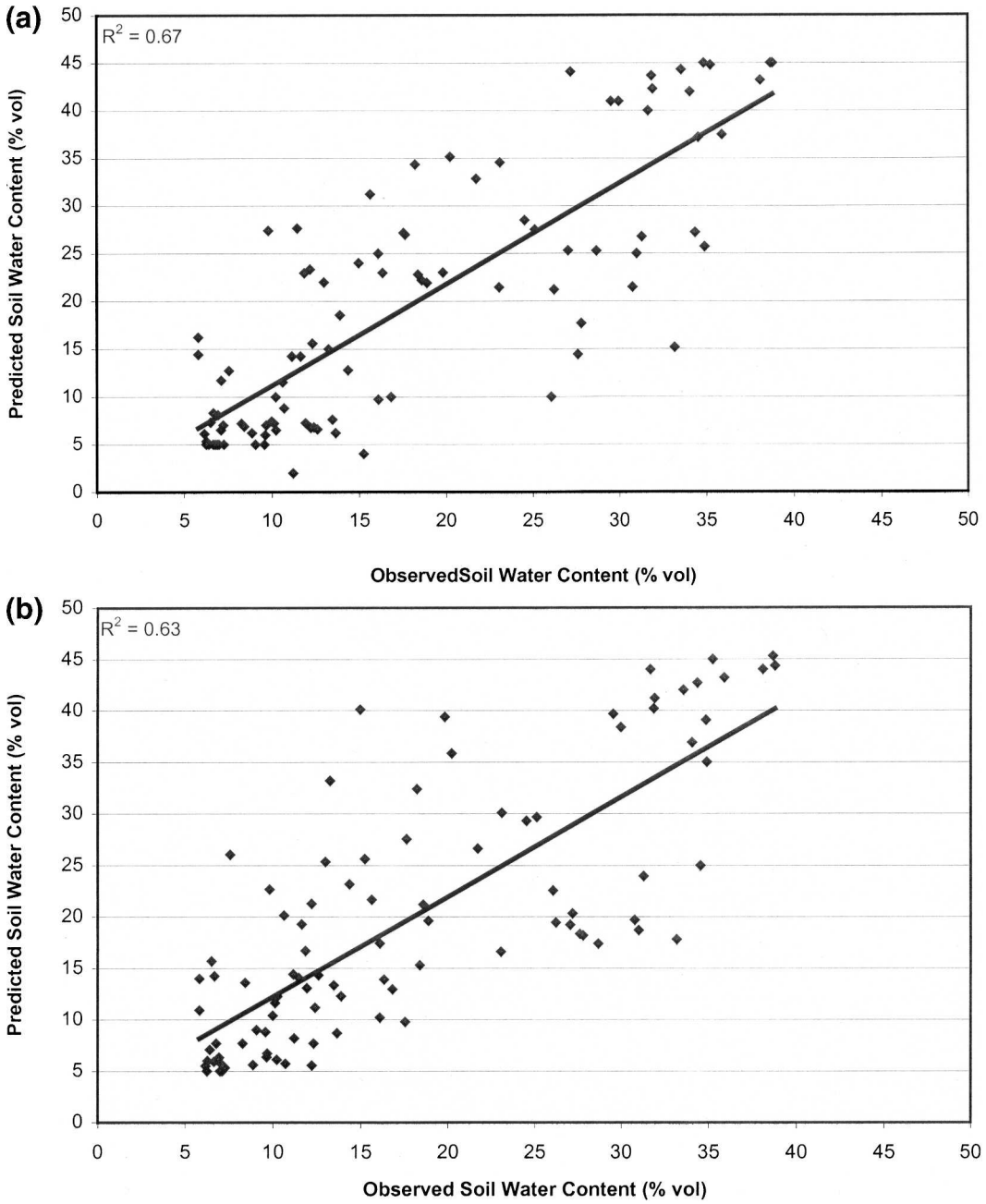

FIG. 10. Observed vs predicted soil water content estimated from trend surfaces of (a) PBL height and (b) 2-m potential temperature change using observations of stability, PBL height, and 2-m potential temperature change.

common parameterizations for A_R should be used with caution. By definition, A_R is proportional to the surface sensible heat flux. Thus, setting A_R equal to a constant can result in substantial errors in estimated entrainment fluxes depending on the magnitude of H_s (Kustas and Brutsaert 1987), which varies diurnally and from day to day. Previous studies have suggested that A_R is seasonal and increases over the summer in the southern Great Plains (Betts and Ball 1994; Margulis and Entekhabi 2004). Our data, however, show that A_R decreases from June through August (as a result of increasing H_s during the summer, which more than offsets the actual increase in H_i). In other words, the total amount of heat brought into the PBL through entrainment increases during the summer, even though it is not reflected in A_R. This condition is further evidenced by a corresponding decline in Δq in the mixed layer (another proxy for entrainment).

6. Conclusions

In this paper we examined 132 days of PBL and land surface data from the ARM-SGP site. Results from conservation analyses show that estimation of daily surface fluxes is not possible using traditional or mean approximations for budget terms. Given these limitations, additional variables were examined and empirical methods of describing these relationships were developed. These methods use observations to predict and explain PBL development and structure and are applicable to individual days on regional scales. Perhaps most important is that the methods presented in this paper are based on easily observable variables (stability, soil moisture, PBL height, and 2-m potential temperature change) relative to those necessary for conservation approaches.

A natural and useful extension to the methods described in this paper provides a simple means to estimate soil water content. Daily observations of soil moisture are extremely difficult to obtain directly, and this method does a good job of estimating soil moisture from routinely measured variables. The integrating nature of the PBL with respect to land surface processes, combined with the close relationship between soil moisture and Bowen ratio, suggests that PBL properties should be diagnostic of regional-scale land surface energy balance. It is expected that this method can be applied to locations other than ARM-SGP. It would require a similar analysis to the one presented here to develop the appropriate relationships for the location in question, and research is currently ongoing to investigate the sensitivity of the approaches developed here to varying surface and atmospheric conditions. The results from this work are also particularly useful from a remote sensing perspective because high-resolution observations of PBL structure are now available from sensors on satellite platforms such as the National Aeronautics and Space Administration (NASA) *Terra* [Moderate-Resolution Imaging Spectroradiometer (MODIS)] and *Aqua* (MODIS and Atmospheric Infrared Sounder) spacecraft. Future research efforts will focus on examining relationships over varied land surface conditions and applying this method to remote sensing data.

Acknowledgments. This work was supported by NASA Headquarters through Earth System Science Fellowship Grant NGT5-30405. Data were obtained from the Atmospheric Radiation Measurement Program sponsored by the U.S. Department of Energy, Office of Science, Office of Biological and Environmental Research, Environmental Sciences Division. Many thanks are given to the reviewers of this manuscript who provided extremely helpful and thorough recommendations and to Guido Salvucci and Bruce Anderson for their comments and suggestions.

REFERENCES

Arya, S. P., 2001: *Introduction to Micrometeorology*. Academic Press, 308 pp.

Barr, A. G., and G. S. Strong, 1996: Estimating regional surface heat and moisture fluxes above prairie cropland from surface and upper-air measurements. *J. Appl. Meteor.,* **35,** 1716–1735.

——, and A. K. Betts, 1997: Radiosonde boundary layer budgets above a boreal forest. *J. Geophys. Res.,* **102,** 29 205–29 212.

Betts, A. K., and J. H. Ball, 1994: Budget analysis of FIFE 1987 sonde data. *J. Geophys. Res.,* **99,** 3655–3666.

——, and A. G. Barr, 1996: First International Satellite Land Surface Climatology Field Experiment 1987 sonde budget revisited. *J. Geophys. Res.,* **101,** 23 285–23 288.

Clapp, R. B., and G. M. Hornberger, 1978: Empirical equations for some soil hydraulic properties. *Water Resour. Res.,* **14,** 601–604.

Cleugh, H. A., and S. B. Grimmond, 2001: Modelling regional scale surface energy exchanges and CBL growth in a heterogeneous, urban-rural landscape. *Bound.-Layer Meteor.,* **98,** 1–31.

——, M. R. Raupach, P. R. Briggs, and P. A. Coppin, 2003: Regional-scale heat and water vapour fluxes in an agricultural landscape: An evaluation of CBL budget methods at OASIS. *Bound.-Layer Meteor.,* **110,** 99–137.

Culf, A. D., 1993: The potential for estimating regional sensible heat flux from convective boundary layer growth. *J. Hydrol.,* **146,** 235–244.

Diak, G. R., 1990: Evaluation of heat flux, moisture flux and aerodynamic roughness at the land surface from knowledge of the PBL height and satellite-derived skin temperatures. *Agric. For. Meteor.,* **52,** 181–198.

——, and T. R. Stewart, 1989: Assessment of surface turbulent fluxes using geostationary satellite surface skin temperature and a mixed layer planetary boundary layer scheme. *J. Geophys. Res.,* **94,** 6357–6373.

——, and M. S. Whipple, 1993: Improvements to models and methods for evaluating the land-surface energy balance and 'effective' roughness using radiosonde reports and satellite-measured 'skin' temperature data. *Agric. For. Meteor.,* **63,** 189–218.

——, and ——, 1994: A note on the use of radiosonde data to estimate the daytime fluxes of sensible and latent heat: A comparison with surface flux measurements from the FIFE. *Agric. For. Meteor.,* **68,** 63–75.

Dolman, A. J., A. D. Culf, and P. Bessemoulin, 1997: Observations of boundary layer development during the HAPEX-Sahel intensive observation period. *J. Hydrol.,* **188–189,** 998–1016.

Driedonks, A. G. M., 1982: Models and observations of the growth of the atmospheric boundary layer. *Bound.-Layer Meteor.,* **23,** 283–306.

Ek, M. B., and A. A. M. Holtslag, 2004: Influence of soil moisture on boundary layer cloud development. *J. Hydrometeor.,* **5,** 86–99.

Findell, K. L., and E. A. B. Eltahir, 2003: Atmospheric controls on

soil moisture–boundary layer interactions. Part I: Framework development. *J. Hydrometeor.,* **4,** 552–569.

Freedman, J. M., D. R. Fitzjaarald, K. E. Moore, and R. K. Sakai, 2001: Boundary layer clouds and vegetation–atmosphere feedbacks. *J. Climate,* **14,** 180–197.

Glazier, J., J. L. Monteith, and M. H. Unsworth, 1976: Effects of aerosol on the local heat budget of the lower atmosphere. *Quart. J. Roy. Meteor. Soc.,* **102,** 95–102.

Hipps, L. E., E. Swiatek, and W. P. Kustas, 1994: Interactions between regional surface fluxes and the atmospheric boundary layer over a heterogeneous watershed. *Water Resour. Res.,* **30,** 1387–1392.

Hubbe, J. M., J. C. Doran, J. C. Liljegren, and W. J. Shaw, 1997: Observations of spatial variations of boundary layer structure over the Southern Great Plains Cloud and Radiation Testbed. *J. Appl. Meteor.,* **36,** 1221–1231.

Key, J. R., and A. J. Schweiger, 1998: Tools for atmospheric radiative transfer: Streamer and FluxNet. *Comput. Geosci.,* **24,** 443–451.

Kustas, W. P., and W. Brutsaert, 1987: Virtual heat entrainment in the mixed layer over very rough terrain. *Bound.-Layer Meteor.,* **38,** 141–157.

Lhomme, J.-P., B. Monteny, and P. Bessemoulin, 1997: Inferring regional surface fluxes from convective boundary layer characteristics in a Sahelian environment. *Water Resour. Res.,* **33,** 2563–2569.

Margulis, S. A., and D. Entekhabi, 2004: Boundary-layer entrainment estimation through assimilation of radiosonde and micrometeorological data into a mixed-layer model. *Bound.-Layer Meteor.,* **110,** 405–433.

Oke, T. R., 1987: *Boundary Layer Climates*. Methuen, 435 pp.

Peters-Lidard, C. D., and L. H. Davis, 2000: Regional flux estimation in a convective boundary layer using a conservation approach. *J. Hydrometeor.,* **1,** 170–182.

Pino, D., J. V.-G. Arellano, and P. G. Duynkerke, 2003: The contribution of shear to the evolution of a convective boundary layer. *J. Atmos. Sci.,* **60,** 1913–1926.

Smith, E. A., and Coauthors, 1992: Area-averaged surface fluxes and their time-space variability over the FIFE experimental domain. *J. Geophys. Res.,* **97,** 18 599–18 622.

Stull, R. B., 1988: *An Introduction to Boundary Layer Meteorology*. Kluwer Academic, 670 pp.

Swiatek, E., 1992: Estimating regional surface fluxes from measured properties of the atmospheric boundary layer in a semiarid ecosystem. M.S. thesis, Dept. of Plants, Soils, and Biometeorology, Utah State University, 119 pp.

Tennekes, H., 1973: A model for the dynamics of the inversion above a convective boundary layer. *J. Atmos. Sci.,* **30,** 558–567.

Venables, W. N., and B. D. Ripley, 1999. *Modern Applied Statistics with S-PLUS*. Springer, 382 pp.

Yi, C., K. J. Davis, and B. W. Berger, 2001: Long-term observations of the dynamics of the continental planetary boundary layer. *J. Atmos. Sci.,* **58,** 1288–1299.